Structures and Magnetic Susceptibility Studies of Four New High-Nuclearity Copper(II) Halide Oligomers

M. R. Bond, H. Place, Z. Wang, and R. D. Willett*

Department of Chemistry, Washington State University, Pullman, Washington 99164

Ying Liu, Todd E. Grigereit, John E. Drumheller,* and George F. Tuthill

Department of Physics, Montana State University, Bozeman, Montana 59717

Received January 11, 1995[⊗]

The syntheses, crystal structures, and powder magnetic studies of several new quasi-planar bibridged $Cu_nX_{2n+2}^{2-}$ oligomers (n = 3, 4, 6, and 7; X = Cl or Br) are reported, based on the 1-methylpyridinium $(C_6H_8N)^+$ and 1,2-dimethylpyridinium $(C_7H_{10}N)^+$ cations. These include $(C_7H_{10}N)_2Cu_3Br_8$, $(C_6H_8N)_2Cu_4Cl_{10}$, $(C_7H_{10}N)_2Cu_6Cl_{14}$, and $(C_7H_{10}N)_2Cu_7Br_{16}$. Crystallographic data: $(C_7H_{10}N)_2Cu_3Br_8$, triclinic, space group $P\bar{1}$, a = 7.947(2) Å, b = 8.799(2) Å, c = 9.840(2) Å, α = 86.95(2)°, β = 76.23(2)°, γ = 71.54(2)°, V = 633.6(3) Å^3, Z = 2, d_x = 2.78 g/cm^3, and R = 0.0483; $(C_6H_8N)_2Cu_4Cl_{10}$, monoclinic, space group $P2_1/n$, a = 11.759(2) Å, b = 9.056(2) Å, c = 12.048(3) Å, β = 106.21(2)°, V = 1232.1(5) Å^3, Z = 2, d_x = 2.15 g/cm^3, and R = 0.0321; $(C_7H_{10}N)_2Cu_6Cl_{14}$, triclinic, $P\bar{1}$, a = 8.997(3) Å, b = 9.288(3) Å, c = 11.540(4)Å, α = 80.53(2)°, β = 67.82(2)°, γ = 60.22(2)°, V = 714.7(4) Å^3, Z = 1, d_x = 2.34 g/cm^3, and R = 0.0363; $(C_6H_8N)_2Cu_7Br_{16}$, triclinic, $P\bar{1}$, a = 7.237(2) Å, b = 10.880(2) Å, c = 12.880(2) Å, α = 89.47(2)°, β = 75.08(2)°, γ = 79.48(2)°, V = 962.7(3) Å^3, Z = 1, d_x = 3.35 g/cm^3, and R = 0.0520. A common feature of the structures is the existence of oligomers containing quasi-planar symmetric bibridged finite chains of edge-sharing CuX_4 (X = halide) monomeric units. The n = 3 oligomers aggregate into chains through the formation of asymmetric bibridged linkages between terminal copper ions on adjacent trimers. In the n = 4 salt, the oligomers aggregate into stacks in which pairs of the copper ions extend their coordination sphere by forming a long, semicoordinate bond to a halide ion from a neighboring oligomer. For both the n = 3 and n = 4 salts, the pyridinium cations lie parallel to and directly above and below the anionic oligomers, separating the chains. In the n = 6 and n = 7 salts, the stacks formed in this manner interdigitate, forming two-dimensional slabs. The slabs are separated by the organic cations. The magnetic properties of compounds are dominated by antiferromagnetic intraoligomer interactions. Thus, the n = 4 and n = 6 salts depopulate into singlet ground states at low temperature. In contrast, the n = 3 and n = 7 oligomers have $S = {}^1/_2$ ground states. Expressions for the magnetic susceptibility of the n = 6 and n = 7 oligomers were obtained by diagonalization of a nearest neighbor Heisenberg Hamiltonian. The data were fit to these expressions, with inclusion of a mean field correction for interoligomer exchange. The intra-oligomer exchange coupling constants are J_1/k = −153 K for n = 3; J_1/k = −60 K, J_2/k = −40 K for n = 4; J_1/k = −23 K, J_2/k = −30 K, and J_3/k = −52 K for n = 5 and J_1/k = −90 K, J_2/k = −90 K and J_3/k = −120 K. At low temperature, the n = 3 oligomer exhibits ferromagnetic behavior. Since the oligomer has depopulated to a spin ${}^1/_2$ ground state, the system can be modeled as a spin ${}^1/_2$ ferromagnetic chain with J'/k = 22.8 K.

Introduction

Much of the work in our laboratories has centered around the structural and magnetic properties of a homologous series of complex ions or molecules with stoichiometry $Cu_nX_{2n}L_2$ (X = halide, L = halide or neutral ligand). The building block of this system is the monomeric CuX_2L_2 species with approximately square planar geometry. The higher oligomers ($n \geq 2$) are quasi-planar chains of edge-sharing CuX_2L_2 monomers with two halide bridges between neighboring copper(II) ions. These oligomers frequently aggregate into stacks in which the copper ion completes its coordination sphere by forming long, semicoordinate bonds to chloride ions on either one or two neighboring oligomers. The formation of the semicoordinate bonds requires a relative displacement of neighboring oligomers which varies in some periodic manner as one proceeds along the stack. We have recently reviewed the surprising variety of such stacking patterns found among these compounds.[1]

The single unpaired electron of the copper(II) ion occupies the $d_{x^2-y^2}$ orbital and is primarily delocalized onto the four equatorial ligands. Consequently the intraoligomer exchange interaction is generally much stronger than the interoligomer exchange interaction providing good examples of finite spin-${}^1/_2$ chains. The dimeric systems have been the most intensely studied since they provide the simplest magnetically coupled systems (in addition to being the most numerous of the spin-${}^1/_2$ systems). The dimeric systems have proved particularly useful in elucidating correlations between structural parameters of the dimer and observed magnetic properties.[2] The trimeric systems have generated some interest recently since certain trimer stacking patterns permit competing interoligomer exchange interactions resulting in a partial spin frustration within the

[⊗] Abstract published in *Advance ACS Abstracts,* May 1, 1995.

(1) Bond, M. R., Willett, R. D. *Inorg. Chem.* **1989**, *28*, 3267. Willett, R. D. *Acta Crystallogr.* **1993**, *A49*, 613.

(2) Willett, R. D. *Magneto-Structural Correlations in Exchange Coupled Systems*; Willett, R. D., Gatteschi, D., Kahn, O. Eds.; D. Reidel: Dordrecht, The Netherlands, 1985; p 389.

0020-1669/95/1334-3134$09.00/0

Table 1. Crystal Structure Conditions and Parameters

	1,2-DMPCu3B	1-MPCu4C	1,2-DMPCu6C	1,2-DMPCu7B
empirical formula	$C_{14}H_{20}Br_8Cu_3N_2$	$C_{12}H_{16}Cl_{10}Cu_4N_2$	$C_{14}H_{20}Cl_{14}Cu_6N_2$	$C_{14}H_{20}Br_{16}Cu_7N_2$
mol wt	1046.22	796.99	1093.94	1939.61
cryst class	triclinic	monoclinic	triclinic	triclinic
space group	$P\bar{1}$	$P2_1/n$	$P\bar{1}$	$P\bar{1}$
a, Å	7.947(2)	11.759(2)	8.997(3)	7.237(2)
b, Å	8.799(2)	9.056(2)	9.288(3)	10.880(2)
c, Å	9.840(2)	12.048(3)	11.540(4)	12.880(2)
α, deg	86.95(2)	90	80.53(2)	89.47(2)
β, deg	76.23(2)	106.21(2)	67.82(2)	75.08(2)
γ, deg	71.54(2)	90	60.22(2)	79.48(2)
vol, Å^3	633.7(4)	1232.1(5)	774.7(4)	962.7(3)
radiation	Mo Kα(λ = 0.710 69 Å)	Mo Kα(λ = 0.710 69 Å)	Mo Kα(λ = 0.710 69 Å)	Mo Kα(λ = 0.710 69 Å)
μ, cm^{-1}	151	45.21	53.0	202.70
ϱ_{calc}, g/cm^3	2.74	2.15	2.34	3.35
Z	2	2	1	1
$R = \sum\|\|F_o\| - \|F_c\|\|/\sum\|F_o\|$	0.0483	0.0321	0.0363	0.0597
$R_w = \sum w(\|F_o\| - \|F_c\|)^2/\sum w\|F_o\|^2$	0.0600	0.0383	0.0458	0.0776

stack.[3] Studies of higher nuclearity oligomers are in short supply primarily because only a few have been synthesized to date. Crystal structures and magnetic susceptibility studies of a few tetramers have been completed[4] and a crystal structure of a pentamer (previously the longest known oligomer) has been determined.[5]

A number of basic correlations have been obtained from studies on the quasi-planar Cu_nX_{2n+2} oligomers. In particular, the terminal Cu−X distances were substantially shorter than bridging Cu−X distances. The effect of the short terminal Cu−X distances is to produce a strong alternation in the bridging distances and, to a lesser extent, in the bridging angles. These effects are manifested in systematic variations in the exchange coupling between the copper ions in the oligomers.

In this paper we report the structures and magnetic behavior of four new high-nuclearity oligomers: bis(1,2-dimethylpyridinium) octabromotricuprate(II) (1,2-DMPCu3B), bis(1-methylpyridinium) decachlorotetracuprate(II) (1-MPCu4C), bis(1,2-dimethylpyridinium) tetradecachlorohexacuprate(II) (1,2-DMPCu6C), and bis(1,2-dimethylpyridinium) hexadecachloroheptacuprate(II) (1,2-DMPCu7B). The latter two compounds are significant since they represent the longest oligomers synthesized to date. Magnetically the higher-nuclearity oligomers are interesting since they lie between the smaller dimer and trimer systems, for which exact theoretical models may be easily derived, and the infinite chain systems, for which exact theoretical predictions may be impossible to obtain. Interest has been expressed in developing systems of isolated finite chains with which to test numerical calculations and to study finite chain effects in linear chains.[6] The interactions between oligomers, which lead to the multitude of stacking patterns mentioned above, also have interesting magnetic consequences. Multiple exchange pathways are defined between oligomers which may lead to competing magnetic interactions. Thus, the possibility of spin frustration exists in these systems.[7]

Experimental Section

Synthesis. Organic cation chlorides were prepared by reaction of the appropriate substituted pyridine with methyl chloride using the method of Carpio et al., for quaternization of pyridine.[8] The crystals were grown by slow evaporation of concentrated hydrohalic acid solutions initially equimolar in substituted pyridinium chloride and the appropriate copper(II) halide. The bromide salts were recrystallized three times from concentrated hydrobromic acid. Initial crystallization yielded the heptamer, later crystals obtained proved to be the trimer containing material. Dimeric species with formula $ACu_2Cl_5(H_2O)$ co-crystallized with the 1-methylpyridinium and 1,2-dimethylpyridinium chloride salts.[1,9] Subsequent recrystallization with excess copper(II) halide favored the formation of the higher oligomers.

Structure Determination. Diffraction data were collected at room temperature (295 K) with Mo Kα radiation (λ = 0.710 69 Å) on a Syntex $P2_1$ diffractometer equipped with a graphite monochrometer which has been upgraded to Nicolet P3F specifications. Lattice constants were determined from a least-squares refinement of the angular settings of 25 well-centered reflections[10] with 20° ≤ 2θ ≤ 26° for 1,2-DMPCu3B, 35° ≤ 2θ ≤ 39° for 1-MPCu4C and 1,2-DMPCu6C, and 39° ≤ 2θ ≤ 45° for 1,2-DMPCu7B. A listing of experimental conditions and parameters is presented in Table 1. *Lp* and crystal decay corrections were applied to the data as were empirical absorption corrections. Structures were solved via direct methods and the structures refined using a block-cascade least-squares method. All structure solution and refinement occurred in the context of the SHELXTL package of programs.[11] The function minimized in the least-squares refinement is $\sum w(|F_o| - |F_c|)^2$ where $w = 1/[\sigma^2(F) + gF^2]$ with g = 0.00116, 0.00027, 0.00048, and 0.00200 for 1,2DMPCu3B, 1-MPCu4C, 1,2-DMPCu6C, and 1,2-DMPCu7B, respectively. Atomic coordinates not identified from the initial *E*-map were located on subsequent electron-density difference maps. Anisotropic thermal parameters were refined for all non-hydrogen atoms. Hydrogen atom positions were calculated and constrained through the remaining cycles of refinement to C−H and N−H distances of 0.96 Å and an idealized geometry. Common isotropic thermal parameters were refined for the groups of ring and methyl hydrogen atoms, except for 1,2-DMPCu3B, where the hydrogen U value was set to a value 20% larger than the U value for the corresponding heavy atom. Extinction problems were found with all four crystals and an isotropic extinction correction of the form $F^* = F_c[1.0 + 0.002\chi F^2/(\sin 2\theta)]^{0.25}$ was applied to the data where the value of χ refined to 0.00058(2), 0.0037(2), 0.0052(2), and 0.0019(2) for 1,2-DMPCu3B, 1-MPCu4C, 1,2-DMPCu6C, and 1,2-DMPCu7B, respectively. Atomic coordinates, bond lengths, and bond angles are listed in Tables 2−4 respectively. Further details of the individual structure determinations follow.

(3) Grigereit, T. E., Ramakrishna, B. L., Place, H., Willett, R. D., Pellacani, G. C., Manfredini, T., Menabue, L., Bonamartini-Corradi, A., Battaglia, L. G. *Inorg. Chem.* **1987**, *26*, 2235. Zaspel, C. E., Rubenacker, G. V., Hutton, S. L., Drumheller, J. E., Rubins, R. S., Willett, R. D., Bond, M. R. *J. Appl. Phys.* **1988**, *63*, 3028.

(4) Halvorson, K. E., Grigereit, T., Willett, R. D. *Inorg. Chem.* **1987**, *26* 1716 and references therein.

(5) Willett, R. D., Rundle, R. E. *J. Chem. Phys.* **1964**, *40*, 835.

(6) Palacio, F., Coronado, E., Darriet, J., Drillion, M., Ferey, G., Gatteschi, D., Georges, R., Kopinga, K., Massa, W., Rey, P., Rojo, T., Soos, Z., Torrance, J., Verdaguer, M., Villeneuve, G. *Organic and Inorganic Low-Dimensional Crystalline Materials*, edited by P. Delhaes and M. Drillion Plenum: New York, 1986; p 465.

(7) Grigereit, T. E., Willett, R. D. *J. Appl. Phys. 1987, 61*, 3292.

(8) Bond, M. R., Willett, R. D. *Acta Crystallogr., Sect. C* **1987**, *43*, 2304.

(9) Carpio, R. A., King, L. A., Lindstrom, R. E., Nardi, J. C., Hussey, C. L. *J. Electrochem. Soc.* **1970**, *126*, 1644.

(10) Campana, C. F., Shepard, D. F., Litchman, W. M. *Inorg. Chem.* **1981**, *20*, 4039.

(11) Sheldrick, G. M. *SHELXTL Version 5.1 User's Manual* Nicolet Instrument Corp.: Madison, WI (1986).

Table 2. Atomic Coordinates ($\times 10^4$) and Equivalent Isotropic Thermal Parameters ($Å^2 \times 10^3$)

	x	*y*	*z*	*U*
I. Bis(1,2-dimethylpyridinium) Octabromotricuprate(II)				
Cu(1)	3060(2)	−3574(1)	1106(1)	38(1)
Cu(2)	0	0	0	38(1)
Br(1)	3744(2)	−4087(1)	3358(1)	49(1)
Br(2)	3609(1)	−6354(1)	591(1)	41(1)
Br(3)	2023(2)	−627(1)	1557(1)	53(1)
Br(4)	961(2)	−2807(1)	−513(1)	46(1)
N(11)	−7654(11)	2119(9)	6644(9)	41(3)
C(12)	−7911(13)	1425(12)	5557(10)	35(4)
C(13)	−7265(15)	−233(12)	5436(12)	51(5)
C(14)	−6408(16)	−1123(13)	6402(15)	65(6)
C(15)	−6172(16)	−388(16)	7478(13)	62(6)
C(16)	−6786(16)	1256(13)	7584(12)	53(5)
C(17)	−8348(16)	3885(12)	6841(12)	55(5)
C(18)	−8802(17)	2472(14)	4499(12)	61(5)
II. Bis(1-methylpyridinium) Decachlorotetracuprate(II)				
Cu(1)	268(1)	1800(1)	9858(1)	30(1)
Cu(2)	1649(1)	5080(1)	-94(1)	27(1)
Cl(1)	58(1)	236(1)	1295(1)	40(1)
Cl(2)	1198(1)	3064(1)	8707(1)	32(1)
Cl(3)	843(1)	3704(1)	1136(1)	35(1)
Cl(4)	2133(1)	955(1)	6047(1)	44(1)
Cl(5)	1816(1)	7065(1)	1049(1)	34(1)
N	869(3)	6936(3)	5681(3)	33(1)
C(1)	1391(4)	5607(4)	5914(4)	39(1)
C(2)	1811(4)	4911(5)	5114(4)	48(2)
C(3)	1720(4)	5560(5)	4069(4)	48(2)
C(4)	1189(4)	6919(5)	3848(3)	47(2)
C(5)	763(3)	7586(5)	4666(3)	40(1)
C(6)	425(4)	7697(5)	6563(4)	53(2)
III. Bis(1,2-dimethylpyridinium) Tetrachlorohexacuprate(II)				
Cu(1)	−5975(1)	3749(1)	−607(1)	24(1)
Cu(2)	−2053(1)	1126(1)	−198(1)	23(1)
Cu(3)	−9817(1)	6657(1)	−1236(1)	23(1)
Cl(1)	−8826	5799(1)	514(1)	24(1)
Cl(2)	−3002(1)	2187(1)	−1852(1)	28(1)
Cl(3)	−4913(1)	2973(1)	1021(1)	28(1)
Cl(4)	−6870(1)	4701(1)	−2285(1)	26(1)
Cl(5)	−12638(1)	8475(1)	−9(1)	27(1)
Cl(6)	−10312(1)	7320(1)	−3052(1)	38(1)
Cl(7)	956(1)	−505(1)	−1427(1)	22(1)
N	−3207(3)	7768(3)	4114(2)	32(1)
C(2)	−4115(4)	7112(3)	5058(2)	28(1)
C(3)	−5940(4)	7702(4)	5282(3)	43(2)
C(4)	−6813(5)	8903(4)	4563(4)	49(2)
C(5)	−5863(5)	9522(4)	3598(4)	47(2)
C(6)	−4059(4)	8968(4)	3387(3)	37(1)
C(7)	−1220(4)	7149(4)	3830(3)	40(1)
C(8)	−3108(5)	5751(4)	5795(3)	47(2)
IV. Bis(1,2-dimethylpyridinium) Hexadecabromoheptacuprate(II)				
Cu(1)	10000	5000	5000	48(1)
Cu(2)	8314(3)	4663(2)	2711(1)	40(1)
Cu(3)	7642(3)	4170(2)	151(1)	41(1)
Cu(4)	6699(3)	3602(2)	7607(1)	40(1)
Br(1)	8866(2)	6389(1)	3704(1)	41(1)
Br(2)	9492(2)	3305(1)	3984(1)	40(1)
Br(3)	7882(2)	5965(1)	1180(1)	38(1)
Br(4)	8599(2)	2871(1)	1511(1)	42(1)
Br(5)	6818(2)	5419(1)	−1278(1)	39(1)
Br(6)	7401(2)	2387(1)	9142(1)	42(1)
Br(7)	4345(2)	5002(1)	3653(1)	43(1)
Br(8)	6893(3)	1722(1)	6668(1)	55(1)
N	5116(17)	900(10)	2469(9)	47(5)
C(1)	6744(19)	37(11)	2138(11)	37(5)
C(2)	7962(25)	−216(14)	2771(15)	70(8)
C(3)	7519(29)	416(16)	3755(15)	76(9)
C(4)	5885(29)	1280(15)	4082(14)	67(8)
C(5)	4693(24)	1527(14)	3406(13)	56(7)
C(6)	3821(24)	1149(15)	1751(13)	64(7)
C(7)	7201(24)	−603(15)	1076(15)	75(8)

[a] The equivalent isotropic *U* is one-third the trace of the orthogonalized $\mathbf{U}_{ij}$ tensor.

1,2-Dimethylpyridinium Octabromotricuprate(II) (1,2-DMPCu3B). Measurements were made on a crystal 0.25 × 0.24 × 0.28 mm in size. A total of 1851 data were collected in the range $0 \le h \le 7$, $-8 \le k \le 8$, $-10 \le l \le 10$. Intensities of equivalent reflections (1668 unique) were averaged ($R_{merge} = 0.0284$), of which 1440 had $|F| > 3\sigma(F)$. The final *R* value was 0.048 for 125 parameters. Excursions on the final difference map ranged from −1.4 to +0.8 e/Å^3.

1-Methylpyridinium Decachlorotetracuprate(II) (1-MPCu4C). Measurements were made on a crystal 0.25 × 0.27 × 0.50 mm in size. A total of 2443 data were collected in the range $0 \le h \le 14,0 \le k \le 11$, and $-15 \le l \le 15$. Intensities of equivalent reflections (2172 unique) were averaged ($R_{merge} = 0.0142$), of which 1986 had $|F| > 3\sigma(F)$. Systematic extinctions uniquely identify the space group as centrosymmetric $P2_1/n$. Peaks corresponding to the hydrogen atoms were visible on the difference map. The final *R* value was 0.032 for 130 parameters. Excursions on the final electron-density difference map range from −0.386 to +0.854 e/Å^3.

1,2-Dimethylpyridinium Tetradecachlorohexacuprate(II) (1,2-DMPCu6C). Measurements were made on a crystal 0.30 × 0.33 × 0.41 mm in size. A total of 5849 data were collected in the range $14 \le h \le 14$, $-15 \le k \le 15$, and $0 \le l \le 18$. Intensities of equivalent reflections (5604 unique) were averaged ($R_{merge} = 0.0224$), of which 4648 had $|F| > 3\sigma(F)$. Intensity statistics suggest that the space group is centrosymmetric and structure refined normally in the space group $P\bar{1}$. The nitrogen atom was assigned to the methylated ring atom which is closer to a chloride ion. Since both methylated ring atoms are close to chloride ions, the assignment is somewhat ambiguous; the relative magnitude of their thermal parameters, however, does not contradict the current assignment. The final *R* value was 0.036 for 166 parameters. Excursions on the final electron-density difference map range from −0.58 to +0.85 e/Å^3.

1,2-Dimethylpyridinium Hexadecabromoheptacuprate(II) (1,2-DMPCu7B). Measurements were made on a crystal 0.21 × 0.27 × 0.31 mm in size. A total of 2813 data were collected in the range $0 \le h \le 8$, $-12 \le k \le 12$, and $-14 \le l \le 14$. Intensities of equivalent reflections (2564 unique) were averaged ($R_{merge} = 0.0520$), of which 1984 had $|F| > 3\sigma(F)$. Intensity statistics suggest that the structure is centrosymmetric and the structure refined normally in $P\bar{1}$. The nitrogen position was assigned using the same criterion used for the chloride salt. A final *R* value of 0.060 was obtained for 181 parameters. Excursions on the final electron-density difference map range from −1.27 to 1.45 e/Å^3.

Magnetic Measurements. Magnetic susceptibility data on powder samples of the above compounds were obtained on an EG&G PAR vibrating sample magnetometer at field strength of 5000 K.

Structure Descriptions

1,2-DMPCu3Br and 1-MPCu4C. The structures consist of centrosymmetric $Cu_3Br_8^{2-}$ and $Cu_4Cl_{10}^{2-}$ units respectively and discrete organic cations, as pictured in Figures 1 and 2. The oligomers are found in stacks in which the copper ions of one oligomer form long, semicoordinate bonds to the neighbors. Diagrams of the two stacks, as shown in **I** and **II**, correspond to the stacking pattern symbols $3(^5/_2, {}^1/_2)$ and $4(^5/_2, {}^1/_2)$ in the notation of Geiser et al.[12]

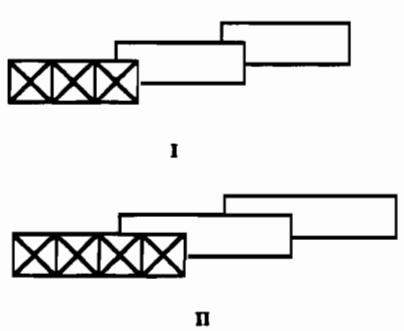

I

II

(12) Geiser, U., Willett, R. D., Lindbeck, M., Emerson, K. *J. Am. Chem. Soc.* **1986**, *108*, 1173.

Table 3. Bond Lengths (Å)

I. Bis(1,2-dimethylpyridinium) Octabromotricuprate(II)[a]							
Cu(1)−Br(1)	2.392(2)	N(11)−C(12)	1.346(15)	Cu(1)−Br(2A)	2.756(2)	C(12)−C(18)	1.507(15)
Cu(1)−Br(2)	2.404(2)	N(11)−C(16)	1.344(15)	Cu(2)−Br(3)	2.399(1)	C(13)−C(14)	1.368(14)
Cu(1)−Br(3)	2.488(2)	N(11)−C(17)	1.481(13)	Cu(2)−Br(4)	2.386(1)	C(14)−C(15)	1.349(21)
Cu(1)−Br(4)	2.492(2)	C(12)−C(13)	1.386(14)	Cu(2)−C(3A)	2.399(1)	C(15)−C(26)	1.374(17)
II. Bis(1-methylpyridinium) Decachlorotetracuprate(II)							
Cu(1)−Cl(2)	2.298(1)	Cu(1)−Cl(1A)	2.303(1)	Cu(2)−Cl(5)	2.239(1)	Cu(2)−Cl(2C)	2.297(1)
Cu(1)−Cl(1B)	2.277(1)	Cu(1)−Cl(3A)	2.284(1)	Cu(2)−Cl(3D)	3.054(1)	Cu(2)−Cl(4E)	2.217(1)
Cu(1)−Cl(5B)	2.600(1)	Cu(2)−Cl(3)	2.330(1)				
N−C(1)	1.345(5)	N−C(5)	1.331(5)	C(2)−C(3)	1.367(7)	C(3)−C(4)	1.372(7)
N−C(6)	1.479(6)	C(1)−C(2)	1.345(7)	C(4)−C(5)	1.365(6)		
III. Bis(1,2-dimethylpyridinium) Tetradecachlorohexacuprate(II)[c]							
Cu(1)−Cl(1)	2.309(1)	Cu(1)−Cl(2)	2.292(1)	Cu(2)−Cl(5A)	2.723(1)	Cu(2)−Cl(7C)	2.301(1)
Cu(1)−Cl(3)	2.278(1)	Cu(1)−Cl(4)	2.255(1)	Cu(3)−Cl(1)	2.373(1)	Cu(3)−Cl(4)	2.304(1)
Cu(1)−Cl(5B)	2.782(1)	Cu(2)−Cl(2)	2.263(1)	Cu(3)−Cl(5)	2.262(1)	Cu(3)−Cl(6)	2.231(1)
Cu(2)−Cl(3)	2.285(1)	Cu(2)−Cl(7)	2.317(1)	Cu(3)−Cl(1B)	2.961(1)	Cu(3)−Cl(7D)	2.998(1)
N−C(2)	1.352(4)	N−C(6)	1.365(4)	C(2)−C(8)	1.495(4)	C(3)−C(4)	1.367(5)
N−C(7)	1.494(4)	C(2)−C(3)	1.377(5)	C(4)−C(5)	1.363(6)	C(5)−C(6)	1.368(6)
IV. Bis(1,2-dimethylpyridinium) Hexabromoheptacuprate(II)							
Cu(1)−Br(1)	2.440(2)	Cu(1)−Br(2)	2.406(2)	Cu(3)−Br(5)	2.412(2)	Cu(3)−Br(3B)	3.229(2)
Cu(1)−Br(7A)	3.177(2)	Cu(2)−Br(1)	2.429(3)	Cu(3)−Br(5C)	3.130(2)	Cu(3)−Br(6D)	2.402(2)
Cu(2)−Br(2)	2.412(2)	Cu(2)−Br(3)	2.469(2)	Cu(4)−Br(6)	2.478(2)	Cu(4)−Br(8)	2.350(2)
Cu(2)−Br(4)	2.445(2)	Cu(2)−Br(7)	2.772(2)	Cu(4)−Br(1B)	3.221(2)	Cu(4)−Br(3A)	3.230(2)
Cu(3)−Br(3)	2.427(2)	Cu(3)−Br(4)	2.402(2)	Cu(4)−Br(5E)	2.480(2)	Cu(4)−Br(7A)	2.384(2)
N−C(1)	1.340(15)	N−C(5)	1.328(20)	C(1)−C(7)	1.472(23)	C(2)−C(3)	1.382(26)
N−C(6)	1.468(23)	C(1)−C(2)	1.340(25)	C(3)−C(4)	1.343(24)	C(4)−C(5)	1.369(28)

[a] Symmetry key: A = $-x, -y, -z$. [b] Symmetry key: A = $x, y, 1+z$; B = $-x, -y, 1-z$; C = $x, y, -1+z$; D = $-x, 1-y, -z$; E = $\frac{1}{2}-x, \frac{1}{2}-y, \frac{1}{2}+z$; F = $-x, 1-y, 1-z$. [c] Symmetry key: A = $1+x, -1+y, z$; B = $-2-x, 1-y, -z$; C = $-x, -y, -z$; D = $-1+x, 1+y, z$. [d] Symmetry key: A = $1-x, 1-y, 1-z$; B = $2-x, 1-y, -z$; C = $1-x, 1-y, -z$; D = $x, y, -1+z$; E = $2-x, 1-y, 1-z$; F = $x, y, 1+z$; G = $-1+x, y, z$.

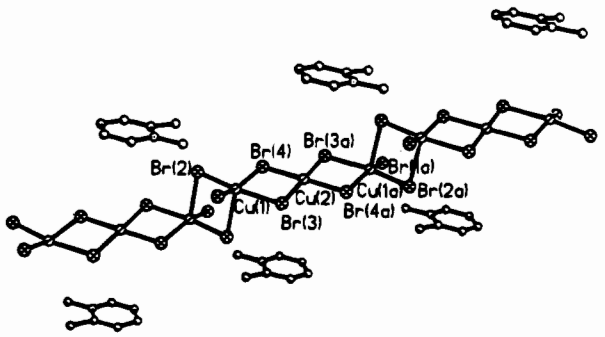

Figure 1. Chain structure in 1,2-DMPCu3Br.

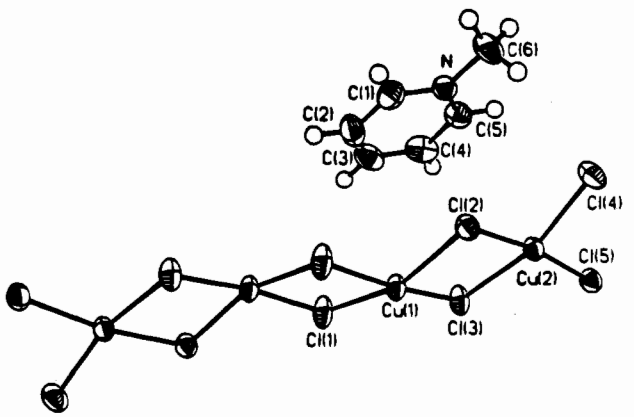

Figure 2. View of the $Cu_4Cl_{10}^{2-}$ anion and $C_6H_8N^+$ cation in the 1-MPCu4C structure.

The general stacking pattern symbol, $n(m_{\parallel}, m_{\perp})$ is defined as follows: n is the number of copper(II) ions in the oligomer and $m_{\parallel}d$ and $m_{\perp}d$ are the translations parallel and perpendicular, respectively, to the Cu−Cu axis of the oligomer necessary to bring the center of one oligomer atop the center of its neighbor in the stack (d is the ligand−ligand distance along the edge of the oligomer). These both correspond to previously unobserved stacking patterns. These unique stacking patterns can be attributed to the presence of the organic cation which is approximately coplanar to the oligomers and located over the oligomer. This prevents the formation of bridging bonds by two of the copper ions in the oligomers and force the unusually large $m_{\parallel} = 5/2$ translation. The proximity of the cation to the anions is effected by an electrostatic interaction between the nitrogen atom of the cation and a halide ion of the tetramer (N−Br(1) = 4.01(2), N−Br(3) = 4.07(2), and N−Br(4) = 4.03(2)Å; N−Cl(2) = 3.47(1)Å). Similar behavior[1,13] is found in several other quaternary pyridinium halometallates.

The Cu(II) ions show subtle differences in geometries in these two structures. In the $Cu_3Br_8^{2-}$ anion, the central copper ion, Cu(2), has a square planar geometry (Cu−Br (average) = 2.392(7)Å). The terminal copper ions, Cu(1), have geometry close to square pyramidal, with the basal plane defined by the four short Cu−Br bonds (2.44(5) Å average) in the oligomer and the axial bond linking to Br(2) in an adjacent trimer. The axial bond distance (Cu(1)−Br(2) = 2.757(2)Å) is significantly shorter than the typical semicoordinate bond. The inequality of the trans $(Br-Cu-Br)_{basal}$ angles indicates a small distortion of the $CuBr_5^{3-}$ species toward a trigonal bipyramidal geometry.

In the $Cu_4Cl_{10}^{2-}$ tetramer, the central pair of copper ions have geometry essentially identical to the end pair in the $Cu_3Br_8^{2-}$. Thus the basal Cu−Cl distances average 2.286 Å with the axial distance (between oligomers) equal to 2.600 Å with similarangular distortions within the basal plane also. The coordination

(13) Prout, C. K., Murray-Rust, P. *J. Chem. Soc. A* **1969** 1520.

Table 4. Bond Angles (deg)[a]

I. Bis(1,2-dimethylpyridinium) Octabromotricuprate(II)

Br(1)−Cu(1)−Br(2)	93.7(1)	C(12)−N(11)−C(16)	122.0(9)	Br(3)−Cu(1)−Br(2A)	94.4(1)	C(14)−C(15)−C(16)	119.3(12)
Br(1)−Cu(1)−Br(3)	91.5(1)	C(12)−N(11)−C(17)	120.1(9)	Br(4)−Cu(1)−Br(2A)	103.4(1)	N(11)−C(16)−C(15)	120.2(12)
Br(2)−Cu(1)−Br(3)	171.1(1)	C(16)−N(11)−C(17)	117.8(10)	Br(3)−Cu(2)−Br(4)	86.7(1)		
Br(1)−Cu(1)−Br(4)	153.9(1)	N(11)−C(12)−C(13)	117.8(9)	Br(4)−Cu(2)−Br(3A)	93.3(1)		
Br(2)−Cu(1)−Br(4)	89.6(1)	N(11)−C(12)−C(18)	119.1(8)	Cu(1)−Br(2)−Cu(1A)	88.5(1)		
Br(3)−Cu(1)−Br(4)	82.5(1)	C(13)−C(12)−C(18)	123.1(10)	Cu(1)−Br(3)−Cu(2)	95.2(1)		
Br(1)−Cu(1)−Br(2A)	102.3(1)	C(12)−C(13)−C(14)	120.6(12)	Cu(1)−Br(4)−Cu(2)	95.5(1)		
Br(2)−Cu(1)−Br(2A)	91.5(1)	C(13)−C(14)−C(15)	120.0(11)				

II. Bis(1-methylpyridinium) Decachlorotetracuprate(II)

Cl(2)−Cu(1)−Cl(1A)	158.3(1)	Cl(2)−Cu(1)−Cl(1B)	93.6(1)	Cl(5)−Cu(2)−Cl(3D)	82.7(1)	Cl(2A)−Cu(2)−Cl(3D)	90.1(1)
Cl(1A)−Cu(1)−Cl(1B)	85.7(1)	Cl(2)−Cu(1)−Cl(3A)	86 .0(1)	Cl(3)−Cu(2)−Cl(4E)	163.1(1)	Cl(5)−Cu(2)−Cl(4E)	94.2(1)
Cl(1A)−Cu(1)−Cl(3A)	91.8(1)	Cl(1B)−Cu(1)−Cl(3A)	172.1(1)	Cl(2C)−Cu(2)−Cl(4E)	91.5(1)	Cl(3D)−Cu(2)−Cl(4E)	110.0(1)
Cl(2)−Cu(1)−Cl(5B)	95.8(1)	Cl(1A)−Cu(1)−Cl(5B)	105.8(1)	Cu(1C)−Cl(1)−Cu(1B)	94.3(1)	Cu(1)−Cl(2)−Cu(2A)	94.7(1)
Cl(1B)−Cu(1)−Cl(5B)	94.9(1)	Cl(3A)−Cu(1)−Cl(5B)	93.0(1)	Cu(2)−Cl(3)−Cu(1C)	94.1(1)	Cu(2)−Cl(3)−Cu(2D)	93.4(1)
Cl(3)−Cu(2)−Cl(5)	91.2(1)	Cl(3)−Cu(2)−Cl(2C)	84.9(1)	Cu(1C)−Cl(3)−Cu(2D)	85.7(1)	Cu(2)−Cl(5)−Cu(1F)	98.5(1)
Cl(5)−Cu(2)−Cl(2C)	172.0(1)	Cl(3)−Cu(2)−Cl(3D)	86.6(1)				

C(1)−N−C(5)	120.5(4)	C(1)−N−C(6)	120.0(3)	C(1)−C(2)−C(3)	120.4(4)	C(2)−C(3)−C(4)	118.6(4)
C(5)−N−C(6)	119.5(3)	N−C(1)−C(2)	120.2(4)	C(3)−C(4)−C(5)	119.7(4)	N−C(5)−C(4)	120.5(4)

III. Bis(1,2-dimethylpyridinium) Tetradecachlorohexacuprate(II)

Cl(1)−Cu(1)−Cl(2)	167.4(1)	Cl(1)−Cu(1)−Cl(3)	95.3(1)	Cl(4)−Cu(3)−Cl(6)	89.3(1)	Cl(5)−Cu(3)−Cl(6)	97.0(1)
Cl(2)−Cu(1)−Cl(3)	86.1(1)	Cl(1)−Cu(1)−Cl(4)	85.4(1)	Cl(1)−Cu(3)−Cl(1B)	87.0(1)	Cl(4)−Cu(3)−Cl(1B)	93.4(1)
Cl(2)−Cu(1)−Cl(4)	91.8(1)	Cl(3)−Cu(1)−Cl(4)	173.4(1)	Cl(5)−Cu(3)−Cl(1B)	85.5(1)	Cl(6)−Cu(3)−Cl(1B)	96.7(1)
Cl(1)−Cu(1)−Cl(5B)	88.9(1)	Cl(2)−Cu(1)−Cl(5B)	103.6(1)	Cl(1)−Cu(3)−Cl(7D)	87.4(1)	Cl(4)−Cu(3)−Cl(7D)	96.9(1)
Cl(3)−Cu(1)−Cl(5B)	92.3(1)	Cl(4)−Cu(1)−Cl(5B)	94.2(1)	Cl(5)−Cu(3)−Cl(7D)	83.5(1)	Cl(6)−Cu(3)−Cl(7D)	90.4(1)
Cl(2)−Cu(2)−Cl(3)	86.6(1)	Cl(2)−Cu(2)−Cl(7)	94.1(1)	Cl(1B)−Cu(3)−Cl(7D)	167.5(1)	Cu(1)−Cl(1)−Cu(3)	94.1(1)
Cl(3)−Cu(2)−Cl(7)	172.9(1)	Cl(2)−Cu(2)−Cl(5A)	94.5(1)	Cu(1)−Cl(1)−Cu(3B)	89.9(1)	Cu(3)−Cl(1)−Cu(3B)	93.0(1)
Cl(3)−Cu(2)−Cl(5A)	98.0(1)	Cl(7)−Cu(2)−Cl(5A)	89.0(1)	Cu(1)−Cl(2)−Cu(2)	93.2(1)	Cu(1)−Cl(3)−Cu(2)	93.0(1)
Cl(2)−Cu(2)−Cl(7C)	168.0(1)	Cl(3)−Cu(2)−Cl(7C)	92.4(1)	Cu(1)−Cl(4)−Cu(3)	97.5(1)	Cu(3)−Cl(5)−Cu(1B)	95.6(1)
Cl(7)−Cu(2)−Cl(7C)	85.4(1)	Cl(5A)−Cu(2)−Cl(7C)	97.5(1)	Cu(3)−Cl(5)−Cu(2D)	98.0(1)	Cu(1A)−Cl(5)−Cu(2D)	166.3(1)
Cl(1)−Cu(3)−Cl(4)	82.8(1)	Cl(1)−Cu(3)−Cl(5)	90.9(1)	Cu(2)−Cl(7)−Cu(2C)	94.6(1)	Cu(2)−Cl(7)−Cu(3A)	89.5(1)
Cl(4)−Cu(3)−Cl(5)	173.6(1)	Cl(1)−Cu(3)−Cl(6)	171.5(1)	Cu(2B)−Cl(7)−Cu(3A)	99.1(1)		

C(2)−N−C(6)	121.3(3)	C(2)−N−C(7)	120.0(3)	C(2)−C(3)−C(4)	121.1(3)	C(3)−C(4)−C(5)	119.7(4)
C(6)−N−C(7)	118.7(3)	N−C(2)−C(3)	118.3(3)	C(4)−C(5)−C(6)	119.5(4)	N−C(6)−C(5)	120.1(3)
N−C(2)−C(8)	119.5(3)	C(3)−C(2)−C(8)	122.2(3)				

IV. Bis(1,2-dimethylpyridinium) Hexadecabromoheptacuprate(II)

Br(1)−Cu−Br(2)	86.9(1)	Br(1)−Cu(1)−Br(7A)	88.7(1)	Br(8)−Cu(4)−Br(3A)	97.6(1)	Br(1A)−Cu(4)−Br(3A)	171.2(1)
Br(2)−Cu(1)−Br(7A)	96.1(1)	Br(1)−Cu(2)−Br(2)	87.0(1)	Br(6)−Cu(4)−Br(5F)	83.7(1)	Br(8)−Cu(4)−Br(5F)	172.1(1)
Br(1)−Cu(2)−Br(3)	93.0(1)	Br(2)−Cu(2)−Br(3)	167.2(1)	Br(1E)−Cu(4)−Br(5F)	88.9(1)	Br(3A)−Cu(4)−Br(5F)	86.1(1)
Br(1)−Cu(2)−Br(4)	166.2(1)	Br(2)−Cu(2)−Br(4)	90.9(1)	Br(6)−Cu(4)−Br(7A)	170.7(1)	Br(8)−Cu(4)−Br(7A)	97.6(1)
Br(3)−Cu(2)−Br(4)	86.0(1)	Br(1)−Cu(2)−Br(7)	95.6(1)	Br(1E)−Cu(4)−Br(7A)	88.6(1)	Br(3A)−Cu(4)−Br(7A)	84.0(1)
Br(2)−Cu(2)−Br(7)	99.7(1)	Br(3)−Cu(2)−Br(7)	93.1(1)	Br(5F)−Cu(4)−Br(7A)	89.7(1)	Cu(1)−Br(1)−Cu(2)	92.4(1)
Br(4)−Cu(2)−Br(7)	98.2(1)	Br(3)−Cu(3)−Br(4)	87.9(1)	Cu(1)−Br(1)−Cu(4E)	90.3(1)	Cu(2)−Br(1)−Cu(4E)	98.0(1)
Br(3)−Cu(3)−Br(5)	93.5(1)	Br(4)−Cu(3)−Br(5)	117.2(1)	Cu(1)−Br(2)−Cu(2)	93.7(1)	Cu(2)−Br(3)−Cu(3)	91.7(1)
Br(3)−Cu(3)−Br(3B)	88.9(1)	Br(4)−Cu(3)−Br(3B)	91.7(1)	Cu(2)−Br(3)−Cu(3B)	100.7(1)	Cu(3)−Br(3)−Cu(3B)	91.1(1)
Br(5)−Cu(3)−Br(3B)	85.9(1)	Br(3)−Cu(3)−Br(5C)	89.3(1)	Cu(2)−Br(3)−Cu(4A)	85.0(1)	Cu(3)−Br(3)−Cu(4A)	91.6(1)
Br(4)−Cu(3)−Br(5C)	94.9(1)	Br(5)−Cu(3)−Br(5C)	87.5(1)	Cu(3B)−Br(3)−Cu(4A)	173.6(1)	Cu(2)−Br(4)−Cu(3)	92.9(1)
Br(3A)−Cu(3)−Br(5C)	173.1(1)	Br(3)−Cu(3)−Br(6D)	179.7(1)	Cu(3)−Br(5)−Cu(3C)	92.5(1)	Cu(3)−Br(5)−Cu(4D)	94.6(1)
Br(4)−Cu(3)−Br(6D)	91.8(1)	Br(5)−Cu(3)−Br(6D)	86.8(1)	Cu(3C)−Br(5)−Cu(4D)	93.0(1)	Cu(4)−Br(6)−Cu(3F)	94.9(1)
Br(3B)−Cu(3)−Br(6D)	91.2(1)	Br(5C)−Cu(3)−Br(6D)	90.6(1)	Cu(2)−Br(7)−Cu(1G)	169.8(1)	Cu(2)−Br(7)−Cu(4A)	97.7(1)
Br(6)−Cu(4)−Br(8)	89.5(1)	Br(6)−Cu(4)−Br(1E)	97.6(1)	Cu(1G)−Br(7)−Cu(4C)	92.4(1)		
Br(8)−Cu(4)−Br(1E)	88.1(1)	Br(6)−Cu(4)−Br(3A)	89.1(1)				

C(1)−N−C(5)	121.5(14)	C(1)−N−C(6)	117.7(12)	C(1)−C(2)−C(3)	119.5(15)	C(2)−C(3)−C(4)	120.7(20)
C(5)−N−C(6)	120.8(12)	N−C(1)−C(2)	119.5(13)	C(3)−C(4)−C(5)	118.7(17)	N−C(5)−C(4)	120.7(14)
N−C(1)−C(7)	119.9(14)	C(2)−C(1)−C(7)	120.6(12)				

[a] Symmetry key: see Table 3 for all four compounds.

geometry of the terminal copper ions is of the folded 4 + 1 type consisting of four short coordinate bonds in the plane of the tetramer and one long, axial semicoordinate bond (Cu(2)−Cl(3D) = 3.054(1) Å) to a chloride ion in a neighboring tetramer. The folded geometry is accompanied by a small tetrahedral distortion of the equatorial plane.

1,2-DMPCu6C and 1,2-DMPCu7B. The structures of these two salts show very similar features, given the fact that the bromide salt contains a heptamer instead of the hexameric unit found in the chloride salt. The structures consists of discrete oligomeric centrosymmetric anions and discrete 1,2-dimethylpyridinium cations as depicted in Figures 3 and 4. The halide ions of the quasi-planar oligomers form long, semicoordinate bonds to four neighboring oligomeric anions. This results in the more complicated interdigitated stacking patterns shown diagramatically in **III** and **IV** and denoted $6[^5/_2, {}^1/_2)][(-^9/_2, -{}^1/_2)]$, and $7[(^7/_2, {}^1/_2)][(-^9/_2, -{}^1/_2)]$.

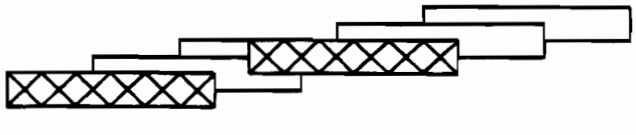

III

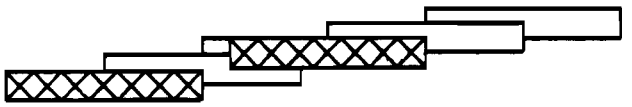

IV

Instead of a single stack in which a given oligomer bonds only to two neighbors, the stacks of oligomers in these two structures are interdigitated to give layers of linked oligomers parallel to the *ab*-planes (hexamer, Figure 5) and the *ac*-plane (heptamer) of the structure.[14]

In contrast to the first two structures, the 1,2-dimethylpyridinium cations are not coplanar to the stacks. Rather, the normal to the cation plane makes an oblique angle to the normal to the central plane of the oligomer (50° in the chloride salt, 51° in the bromide salt) and the cation is excluded from the hexamer stacks as shown in the stereographic diagram of the hexamer structure in Figure 5. The interdigitation of the stacks is favorable energetically since it allows each copper ion to complete its coordination sphere by adding two axial ligands to give a square bipyramidal geometry as pictured in Figure 6. Nevertheless, an electrostatic interaction exist between the nitrogen atom of the cation and Cl(4) of the hexamer (N−Cl = 3.325(4) Å; interaction vector angle = 13°). In the bromide salt the nitrogen cations form close electrostatic interactions with bromide ions in both neighboring layers (N−Br(4) = 3.58(2) Å, interaction vector angle = 14°; N−Br(8) = 3.48(2) Å, interaction vector angle = 10°).

Because of the extensive bonding between oligomers in the $n = 6$ and $n = 7$ salts, there are only small distortions from planarity. The coordination about the Cu(II) ions is either 4 + 2 (four short equitorial bonds and two longer semicoordinate bonds) or 4 + 1 + 1 (four short equatorial bonds, one moderately long semicoordinate axial bond, and one very long semicoordinate axial bond). For example, in the hexamer, the coordination about Cu(1) is 4 + 1 + 1, with $(Cu(1)-Cl_{eq})_{av}$ = 2.28(2) Å, Cu(1)−Cl(5) = 2.781(1) Å, and Cu(1)−Cl(3) = 3.433(1) Å, while Cu(3) has $(Cu(3)-Cl_{eq})_{av}$ = 2.29(6) Å, Cu(3)−Cl(1) = 2.961 (1) Å, and Cu(3)−Cl(7) = 2.998 (1) Å. A more detailed analysis of the coordination geometries is given in ref 15.[15]

The relative planarity of the hexamer compared with the tetrameric 1-MPCu4C implies that the intraoligomer bonding geometry should more readily correspond to the trends observed by Willett.[16] Specifically the bonding parameters within the oligomer are not uniform but in general exhibit an alternation as one moves from the terminus to the center. For instance, if one denotes pairs of Cu−Cl bonds by t, b_1, ..., b_i, ... (where t is the terminal pair of Cu−Cl bonds and b_i is a pair of Cu−Cl bonds to the same Cu atom and numbered sequentially starting with the outermost pair) then the terminal pair, t, should have the shortest average bond length, the neighboring bridging pair, b_1, should have the longest average bond length, and the alternation in bond length will continue, with decreasing amplitude, as one moves toward the center of the oligomer. This trend is approximately followed by the hexamer as shown by the average Cu−Cl bond lengths: t = 2.246 Å, b_1 = 2.339 Å, b_2 = 2.282 Å, b_3 = 2.285 Å, b_4 = 2.274 Å, and b_5 = 2.309 Å.

(14) It is possible to define several possible stacks within this planar aggregation of oligomers which introduces some ambiguity into the stacking pattern notation. This problem is resolved by defining two different stacking patterns which uniquely define the layer structure. In the stacking pattern symbol, then, the two definitive patterns are distinguished from one another by enclosing them in brackets, as written above.

(15) Willett, R. D. *Acta Cryst. B* **1988**, *44*, 503.

(16) Bond, M. R. Ph.D. Thesis, Washington State University, 1990.

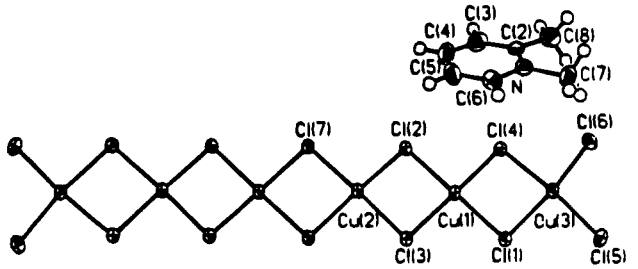

Figure 3. View of the $Cu_6Cl_{14}^{2-}$ anion and $C_7H_{10}N^+$ cation in the 1,2-DMPCu6C structure.

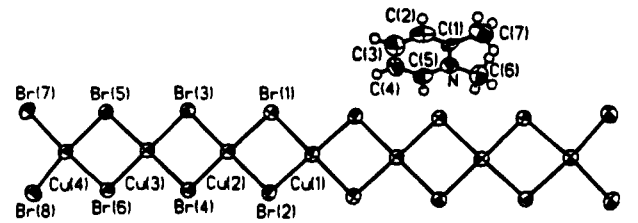

Figure 4. View of the discrete $Cu_7Br_{16}^{2-}$ anion and $C_7H_{10}N^+$ cation of the 1,2-DMPCu7B structure.

Similar behavior is expected for the pairs of bridging Cu−Cl−Cu angles, ϕ_i, numbered sequentially starting with the outermost pair: $\phi_1 = 95.9°$, $\phi_2 = 93.1°$, and $\phi_3 = 94.6°$. The numerical values for the structural parameters do not always agree with those predicted by Willett for a $Cu_6Cl_{14}^{2-}$ species. The numerical predictions, however, represent a statistical average of parameters from several oligomers; thus comparison with these should be made for a series of hexanuclear oligomers, not an individual system.

Structural correlations in $Cu_nBr_{2n+2}^{2-}$ oligomers have not been studied because of the limited number of compounds which have been studied. Nevertheless, the heptamer salt does follow some of the trends found for the chloride oligomers. Within the heptamer the following bond length averages are found: t = 2.367 Å, b_1 = 2.479 Å, b_2 = 2.407 Å, b_3 = 2.457 Å, b_4 = 2.421 Å, and b_5 = 2.423 Å. The bond lengths alternate starting with the shortest at t, however the correlation fails beyond the b_3 pair, possibly because of the strong square pyramidal distortion about Cu(2). The bridging Cu−Br−Cu angles also show an alternation: $\phi_1 = 94.8°$, $\phi_2 = 92.3°$, and $\phi_3 = 93.1°$.

Magnetic Behavior

Since these compounds are described structurally as stacked chains of linear oligomers, an appropriate model for the magnetic susceptibility would first consist of an expression for the isolated oligomer and then account for the interoligomer interaction through an approximation. The spin Hamiltonians take the forms

$$H_{tri} = -2J_1(\hat{S}_1\cdot S_2 + \hat{S}_2\cdot\hat{S}_3) + gu_\beta H\sum_{i=1}^{3}\hat{S}_z \quad (1)$$

$$H_{tet} = -2J_1(\hat{S}_1\cdot\hat{S}_2 + \hat{S}_3\cdot\hat{S}_4) - 2J_2(\hat{S}_2\cdot\hat{S}_3) + gu_\beta H\sum_{i=1}^{4}\hat{S}_z \quad (2)$$

$$H_{hex} = -2J_1(\hat{S}_1\cdot\hat{S}_2 + \hat{S}_5\cdot\hat{S}_6) - 2J_2(\hat{S}_2\cdot\hat{S}_3 + \hat{S}_4\cdot\hat{S}_5) - 2J_3(\hat{S}_3\hat{S}_4) + gu_\beta H\sum_{i=1}^{6}\hat{S}_z^{\,z} \quad (3)$$

$$H_{hep} = -2J_1(\hat{S}_1\cdot\hat{S}_2 + \hat{S}_6\cdot\hat{S}_7) - 2J_2(\hat{S}_2\cdot\hat{S}_3 + \hat{S}_5\cdot\hat{S}_6) - 2J_3(\hat{S}_3\cdot\hat{S}_4 + \hat{S}_4\cdot\hat{S}_5) + gu_\beta H\sum_{i=1}^{7}\hat{S}_z^{\,z} \quad (4)$$

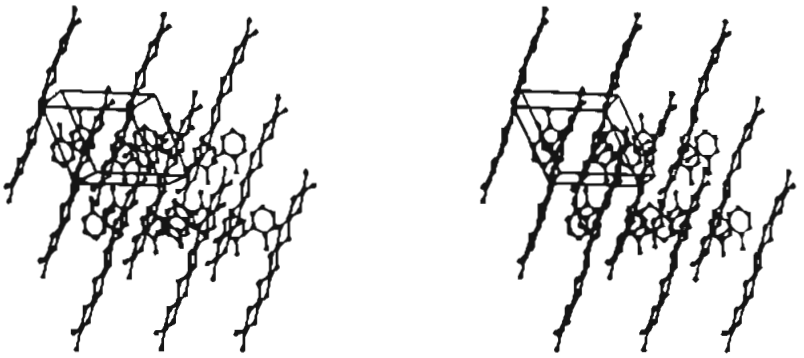

Figure 5. Stereographic view of the 1,2-DMPCu6C structure with the boundaries of the unit cell outlined. The *c*-axis is out of the plane of the paper, the *b*-axis is horizontal, and the *a*-axis is approximately vertical.

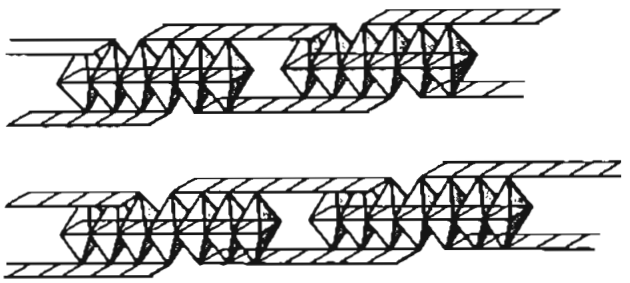

Figure 6. Diagram of the approximately square-bipyramidal coordination of the copper ions (a) 1,2-DMPCu6C and (b) 1,2-DMPCu7B resulting from the interdigitated stacking of the oligomers.

Table 5. Magnetic Parameters

	g	J_1/k (K)	J_2/k (K)	J_3/k (K)	J'/k (K)
1,2-DMPCu3Br	2.07	−153			31
1-MPCu4Cl	2.18	−60	*a*		1
1,2-DMPCu6Cl	2.00	−23	−30	−52	*a*
1,2-DMPCu7Br	2.10	−90	−90	−120	−2

a Value is indeterminate.

where J_1, J_2, and J_3 denote the Cu−Cu exchange constants within the oligomer. A few simplifying assumptions are made in writing the above models: (1) isotropic (Heisenberg) exchange interactions, although copper(II) halide systems typically exhibit a 1−10% exchange anisotropy; (2) equal isotropic g-factors.

Exact solutions are available for $n = 3$ and $n = 4$.[3,4] For $n = 6$ and $n = 7$, the above equations were solved by the numerical calculation of the eigenvalues (E_n) and eigenstates. The expression for the susceptibility is obtained by application of Van Vleck's equation:

$$\chi_c = \frac{N\sum_n [(m_s g u_\beta)^2/kT] \exp(-E_n/kT)}{\sum_n \exp(-E_n/kT)} \quad (5)$$

Interactions between oligomers were taken into account by a mean-field correction which takes the form

$$\chi = \frac{\chi_c}{1 - (2ZJ'\chi_c/Ng^2u_\beta^2)} \quad (6)$$

J' is interoligomer coupling constant and Z is the number of nearest-neighbor oligomer. Results of analyses of the data are given in Table 5. For the $n = 3$ and 4 compounds, parameters were obtained by least squares fitting of the data to these analytical expressions. For $n = 6$ and 7, simulation of the data

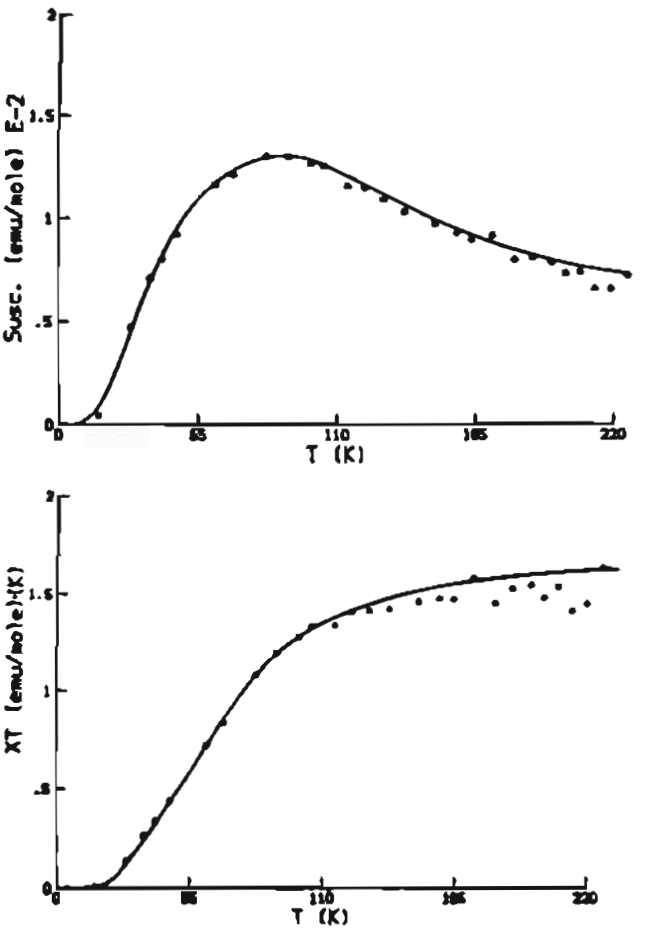

Figure 7. (a) Plot of χ_M vs T for $(C_6H_8N)_2Cu_4Cl_{10}$. (b) Plot of $\chi_M T$ vs T. Dots are experimental values, and the solid line is the theoretical fit (parameters given in Table 5; $J_3/k = -40$ K).

was performed and parameters adjusted to give suitable fits. These results are shown in Figures 7−10.

The $\chi_M T$ vs T plots for all four compounds show decreasing $\chi_M T$ values as T decreases. This is indicative of dominant antiferromagnetic interactions in these systems. These interactions are associated with the exchange coupling within the oligomers. The falloff of $\chi_M T$ is much more rapid for the two bromide salts than for the chloride salts, indicating much stronger exchange coupling in the former. This is in accord with magnetostructural correlations previously elucidated for copper(II) halide compounds[1] and is associated with more effective superexchange in the bromide salts due to the presence of lower lying charge transfer states.

As shown in Figures 7 and 8, the susceptibilities of the chloride tetramer ($n = 4$) and hexamer ($n = 6$) exhibit maxima

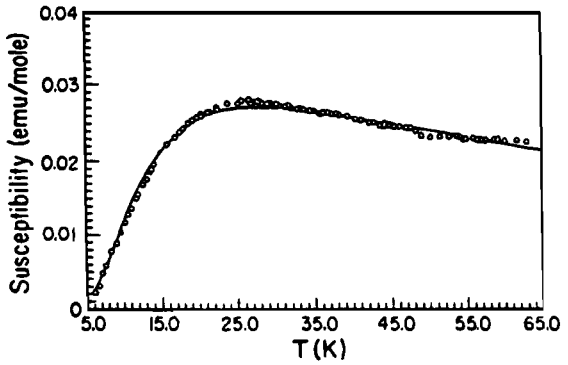

Figure 8. Plot of χ_M vs T for $(C_7H_{10}N)_2Cu_6Cl_{14}$. Circles are experimental values and the solid line is the theoretical fit (parameters given in Table 5; $J' = 0$).

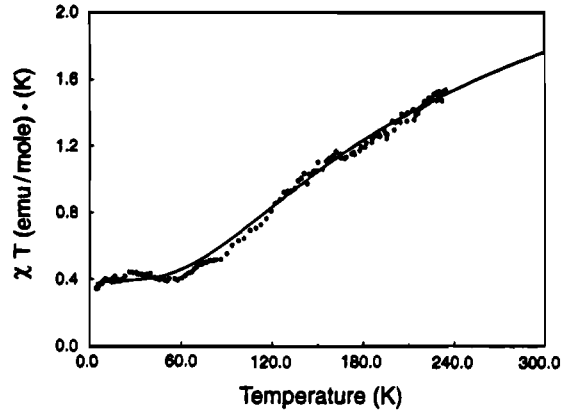

Figure 9. $(C_7H_{10}N)_2Cu_7Br_{16}$ susceptibility data. Dots are experimental values and the solid line is the theoretical fit (parameters in Table 5).

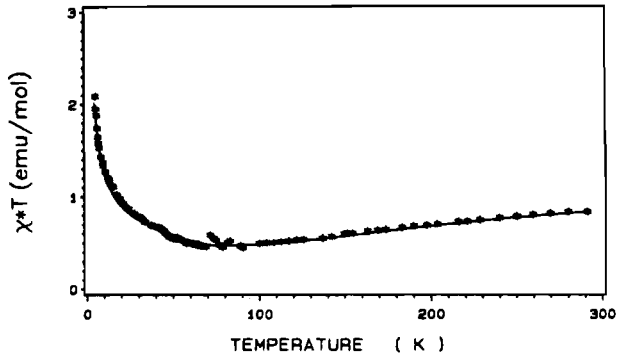

Figure 10. Plot of $\chi_M T$ vs T for $(C_7H_{10}N)_2Cu_3Br_8$. The solid line for $T > 60$ K is the fit to the mean field corrected trimer model. The solid line for $T < 40$ K is the fit to high temperature series expansion for a one-dimensional $S = {}^1/_2$ Heisenberg ferromagnet (parameters given in Table 5).

at $T = 95$ K and $T = 27$ K, respectively, and then fall off to zero as the temperature is lowered. Thus the coupling is significantly weaker in the hexamer than the tetramer. The plot of $\chi_M T$ vs T goes rapidly to zero at low temperature, as seen in Figure 7b for the tetramer. This indicates that the $n = 4$ and 6 oligomers have the $S = 0$ ground state.

The χ_M vs T plot for the $n = 4$ oligomer is fairly sharply peaked, reminiscent of the behavior of an antiferromagnetic dimer system. Thus it is deduced that J_1 is the dominant antiferromagnetic interaction, since it couples Cu(1)−Cu(2) pairs into S = 0 ground states. Least squares fitting of the data for 1-MPCu4Cl to the susceptibility of an isolated linear antiferromagnetic tetramer (eq 2) yielded $J_1/k = -60$ K, with g fixed at 2.18. The value of J_2/k could not be estimated reliably, since its value was very sensitive to the value assumed for g and to the temperature range of data utilized. Similar limitations in the data analysis were observed in previous studies of quasi-planar copper(II) halide tetramers.[4]

In contrast, the χ_M vs T curve for the hexamer has a much broader maximum, indicative that no one exchange coupling dominates. The paramaters obtained from the simulation indicate that the central coupling constant (J_3) is the strongest. However, structural parameters would indicate that the Cu(1)−Cu(2) linkage (the J_2 coupling constant) should be strongest since that has the smallest bridging Cu−Cl−Cu angles and shortest Cu−Cl bond distances. The lack of uniqueness of the simulations does not preclude this possibility.

Modeling of the high temperature data for the $n = 3$ and 7 oligomers reveals stronger coupling in the trimer species ($J_1/k = 153$ K) then in the heptamer ($J_{av}/k = 100$ K). The trimer value is consistent with previous studies.[14] Since the odd spin oligomer eigenstates possess a $S = {}^1/_2$ ground state, the antiferromagnetic coupling in the trimer ($n = 3$) and heptamer ($n = 7$), as shown in Figures 9 and 10, leads to very different low temperature behavior than for the even spin oligomers. In the absence of interoligomer coupling, one expects the value to $\chi_M T$ to approach a constant value of approximately 0.4 at low temperature. Deviations as the temperature approaches zero Kelvin would indicate weak magnetic interactions along or between the chains. For the heptamer ($n = 7$), a slight downturn at the lowest temperature indicates the presence of some net weak antiferromagnetic coupling in the system. In contrast, the product of $\chi_M T$ for the trimer increases rapidly as the temperature decreases below 50 K. This is characteristic of a strong ferromagnetic coupling in the system. Because of the severe lateral displacement of the structure for the trimer $(C_7H_{10}N)_2Cu_3Br_8$ (Figure 1), the appropriate model at low temperatures is that of a simple ferromagnetic chain of $S = {}^1/_2$ particles. The high-temperature expansion[17] for the 1-D FM susceptibility with a mean-field correction was found to be appropriate. The results for the nearest-neighbor exchange constant, J_1/k, interchain coupling constant, J'/k, and g-factor were found to be 22.8 K, 1.5 K, and 2.19 respectively. This result is shown in Figure 10, and has been published elsewhere in more detail.[18] The magnitude of J^1/k is very large compared to the values found in the other oligomers. However, they represent an average value over multiple exchange pathways which, because of the antiferromagnetic intraoligomers exchange, will invariably lead to spin frustration effects.[7] This will lead to an effective interoligomer coupling of ≈0.

Acknowledgment. This work has been supported by NSF Grants DMR 90-11072 and DMR-8803382.

Supplementary Material Available: Tables of anisotropic thermal parameters and derived hydrogen atom positions (5 pages). Ordering information is given on any current masthead page.

IC950029H

(17) Baker, G. V., Rushbrooke, G. S., Jr. *Phys. Res.* **1964**, *135A*, 1272.
(18) Liu, Y., Grigereit, T. E., Drumheller, J. E., Tuthill, G. F., Willett, R. D., Place, H., Bond, M. R. *J. Magn. Magn. Mater.* **1992**, *104−107*.